0026-895X/09/7504-927–937$20.00
MOLECULAR PHARMACOLOGY
Copyright © 2009 The American Society for Pharmacology and Experimental Therapeutics
Mol Pharmacol 75:927–937, 2009

Vol. 75, No. 4
53793/3550676
Printed in U.S.A.

Intracellular Potassium Stabilizes Human *Ether-à-go-go*-Related Gene Channels for Export from Endoplasmic Reticulum[S]

Lu Wang, Adrienne T. Dennis, Phan Trieu, Francois Charron, Natalie Ethier, Terence E. Hebert, Xiaoping Wan, and Eckhard Ficker

Rammelkamp Center for Education and Research, MetroHealth Campus, Case Western Reserve University, Cleveland, Ohio (L.W., A.T.D., X.W., E.F.); and Department of Pharmacology and Therapeutics, McGill University, Montreal, Quebec, Canada (P.T., F.C., N.E., T.E.H.)

Received November 28, 2008; accepted January 12, 2009

ABSTRACT

Several therapeutic compounds have been identified that prolong the QT interval on the electrocardiogram and cause torsade de pointes arrhythmias not by direct block of the cardiac potassium channel human *ether-à-go-go*-related gene (hERG) but via disruption of hERG trafficking to the cell surface membrane. One example of a clinically important compound class that potently inhibits hERG trafficking are cardiac glycosides. We have shown previously that inhibition of hERG trafficking by cardiac glycosides is initiated via direct block of Na^+/K^+ pumps and not via off-target interactions with hERG or any other protein. However, it was not known how pump inhibition at the cell surface is coupled to hERG processing in the endoplasmic reticulum. Here, we show that depletion of intracellular K^+—either indirectly after long-term exposure to cardiac glycosides or directly after exposure to gramicidin in low sodium media—is sufficient to disrupt hERG trafficking. In K^+-depleted cells, hERG trafficking can be restored by permeating K^+ or Rb^+ ions, incubation at low temperature, exposure to the pharmacological chaperone astemizole, or specific mutations in the selectivity filter of hERG. Our data suggest a novel mechanism for drug-induced trafficking inhibition in which cardiac glycosides produce a $[K^+]_i$-mediated conformational defect directly in the hERG channel protein.

The cardiac potassium channel hERG (KCNH2) encodes the α-subunit of the rapid delayed rectifier current I_{Kr}, which plays a central role in terminal repolarization of human ventricular myocytes. Loss of hERG/I_{Kr} function either by inherited mutations or unintentional drug blockade produces long QT syndrome in the clinic and is characterized by a prolongation of the QT interval on the electrocardiogram, an increased propensity for patients to experience syncope and to present with torsades de pointes arrhythmias, or sudden cardiac arrest (Sanguinetti and Tristani-Firouzi, 2006).

Although tremendous progress has been made toward a mechanistic understanding of drug-induced or acquired long QT syndrome (acLQTS) as a result of direct hERG block by a diverse set of small organic molecules (Sanguinetti and Mitcheson, 2005), much less is known about inhibition of hERG trafficking by therapeutic compounds, a novel, more recently discovered mechanism that can also result in

This work was supported by National Institute of Health National Heart, Lung, and Blood Institute [Grant HL71789] and the Canadian Institutes for Health Research.

Article, publication date, and citation information can be found at http://molpharm.aspetjournals.org.

doi:10.1124/mol.108.053793.

[S] The online version of this article (available at http://molpharm.aspetjournals.org) contains supplemental material.

ABBREVIATIONS: hERG, human *ether à-go-go*-related gene; I_{Kr}, rapidly activating delayed rectifier K current; acLQTS, acquired long QT syndrome; ER, endoplasmic reticulum; HEK, human embryonic kidney; WT, wild type; HA, hemaggultinin; HA_{ex}, extracellular hemagglutinin tag; DMEM, Dulbecco's modified Eagle's medium; pH_i, intracellular pH; MEM, minimal essential medium; sf, serum-free; Ch, choline chloride; NMDG, *N*-methyl-D-glucamine; AM, acetoxymethyl ester; BCECF, sodium binding benzofuran isophthalate 2′,7′-bis(carboxyethyl)-5(6′)-carboxyfluorescein; PBFI, K^+ binding benzofuran isophtalate; BN, blue native; PAGE, polyacrylamide gel electrophoresis; ROS, reactive oxygen species; NAC, *N*-acetyl cysteine; MAP, mitogen-activated protein; MEK, mitogen-activated protein kinase kinase; ERK, extracellular signal-regulated kinase; PD98059, 2′-amino-3′-methoxyflavone; fg, fully glycosylated; cg, core glycosylated; U0126, 1,4-diamino-2,3-dicyano-1,4-bis(methylthio)-butadiene; SP600125, anthra [1,9-*cd*]pyrazol-6(2*H*)-one-1,9-pyrazoloanthrone; SB203580, 4-(4-fluorophenyl)-2-(4-methylsulfinylphenyl)-5-(4-pyridyl)1*H*-imidazole; H89, *N*-[2-(4-bromocinnamylamino)ethyl]-5-isoquinoline; KT5720, (9*S*,10*S*,12*R*)-2,3,9,10,11-hexahydro-10-hydroxy-9-methyl-1-oxo-9,12-epoxy-1*H*-diindolo[1,2,3-*fg*:3′,2′,1′-*kl*]pyrrolo[3,4-*i*][1,6]benzodiazocine-10-carboxylic acid hexyl ester; dn, dominant negative; P, peak; BAPTA, 1,2-bis(2-aminophenoxy)ethane-*N*,*N*,*N*′,*N*′-tetraacetic acid.

acLQTS (Ficker et al., 2004; Kuryshev et al., 2005; van der Heyden et al., 2007; Wang et al., 2007). Similar to direct channel block, disruption of hERG trafficking decreases hERG current but on a much slower time scale by reducing channel numbers at the cell surface. Examples for therapeutic compounds that can cause acLQTS by inhibition of hERG trafficking include arsenic trioxide, which is used in the treatment of acute promyelocytic leukemia (Ficker et al., 2004), the antiprotozoical agent pentamidine (Cordes et al., 2005; Kuryshev et al., 2005), the cholesterol-lowering compound probucol (Guo et al., 2007), the antidepressant fluoxetine (Prozac) as well as the antifungal drug ketoconalzole, both of which belong to a potentially large group of compounds that directly block hERG and inhibit channel trafficking at the same time (Wible et al., 2005; Rajamani et al., 2006; Takemasa et al., 2007).

Furthermore, we have reported that cardiac glycosides, which are best known as potent inhibitors of Na^+/K^+ pumps, disrupt hERG trafficking with high specificity and selectivity (Wang et al., 2007). We have shown that long-term exposure to several cardiac glycosides at the nanomolar level, including clinically important digoxin and digitoxin, blocks exit of heterologously expressed hERG from the endoplasmic reticulum (ER). Likewise, cardiac I_{Kr}, the native correlate of hERG, was reduced upon long-term exposure to cardiac glycosides. Most interestingly, however, our previous experiments suggested that hERG trafficking inhibition by cardiac glycosides was not likely to occur via direct interactions with hERG or any closely associated protein necessary for folding or export of hERG from the ER. First, hERG currents were not directly blocked by extracellular application of cardiac glycosides. Second, inhibition of Na^+/K^+ pumps with potassium-free extracellular solutions mimicked the effects of cardiac glycosides on hERG trafficking. Third, overexpression of an ouabain-insensitive rat Na^+/K^+ ATPase subunit was able to attenuate the effect of pump inhibition on hERG trafficking.

The main goal of the present study was to elucidate the molecular mechanism(s) by which cardiac glycosides disrupt hERG channel trafficking. We tested two hypotheses: 1) Na^+/K^+ pump inhibition triggers intracellular signaling pathways that disrupt hERG folding and processing in the ER either via changes in protein phosphorylation and/or gene expression and 2) modification of intracellular ion gradients by pump inhibition adversely affects hERG export from the ER. In our studies, we used hERG channels heterologously expressed in human embryonic kidney (HEK) 293 cells as a model system that allows for extensive manipulation of extracellular as well as intracellular ion composition during incubation with cardiac glycosides. We found that intracellular potassium ions stabilize hERG for export from the ER and propose that depletion of intracellular $[K^+]$ by cardiac glycoside treatment induces a conformational defect directly in hERG.

Materials and Methods

Cell Culture

HEK293 cells stably expressing hERG WT or hERG WT with an extracellular hemagglutinin (HA_{ex}) tag (Ficker et al., 2003, 2004) were maintained at 37°C and 5% CO_2 in DMEM supplemented with 10% fetal bovine serum, L-glutamine, penicillin/streptomycin (DMEM complete medium), and G418 (Geneticin).

To assess the effect of extracellular ion substitutions on hERG processing in the presence and absence of cardiac glycosides, HEK/hERG WT cells were cultured overnight at 37°C and 5% CO_2 in a defined, serum-free 125Na-sf medium (120 mM NaCl, 5 mM KCl, 1 mM $CaCl_2$, 1 mM $MgSO_4$, 0.2 mM NaH_2PO_4, 0.15 mM Na_2HPO_4, 4 mM $NaHCO_3$, 5 mM glucose, 1 mM pyruvic acid, 10 mM lactic acid, and 20 mM HEPES, pH 7.4) supplemented with MEM essential amino acids (Invitrogen, Carlsbad, CA), MEM nonessential amino acids (Invitrogen), and MEM vitamins (Invitrogen). To study the effects of extracellular calcium ions on hERG trafficking, $CaCl_2$ (1 mM) was omitted from 125Na-sf medium to produce 0Ca-sf medium. To study the effects of extracellular sodium ions, 120 mM NaCl was substituted with equimolar concentrations of either choline chloride (Ch-sf) or *N*-methyl-D-glucamine (NMDG-sf). Both Ch-sf and NMDG-sf medium contained approximately 5 mM residual Na^+. In experiments with the cation-selective ionophore gramicidin (Sigma-Aldrich, St. Louis, MO) NMDG-sf medium was used with appropriate concentrations of NMDG substituted by either KCl or RbCl as indicated. Mutant versions of hERG (in pcDNA3) were transiently expressed in HEK293 cells using FuGENE 6 transfection reagent (Roche Diagnostics, Indianapolis, IN) and compared with cells transiently transfected with pcDNA3-hERG WT.

Western Blot Analysis

The polyclonal anti-hERG antibody (rabbit HERG 519) used in the present study has been described previously (Ficker et al., 2003, 2004). In brief, HEK/hERG cells were solubilized for 1 h at 4°C in lysis buffer containing 150 mM NaCl, 1 mM EDTA, 50 mM Tris, pH 8.0, 1% Triton X-100, and protease inhibitors (Complete; Roche Diagnostics). Protein concentrations were determined by the bicinchoninic acid method (Pierce Chemical, Rockford, IL). Proteins were separated on SDS polyacrylamide gels, transferred to polyvinylidene difluoride membranes, and developed using HERG 519 antibody followed by horseradish peroxidase-conjugated secondary antibody and ECL Plus (GE Healthcare, Chalfont St. Giles, Buckinghamshire, UK). For quantitative analysis, signals were captured directly on a Storm PhosphorImager (GE Healthcare).

Measurement of Intracellular Free Ion Concentrations and pH_i

$[Ca^{2+}]_i$/Fura-2. HEK/hERG cells were treated overnight with increasing concentrations of digoxin either in 125Na-sf or 0Ca-sf medium. Cells were harvested and resuspended in ECS solution containing 20 μM Fura-2 AM, the ratiometric Ca^{2+} indicator (Invitrogen; ECS: 140 mM NaCl, 5.4 mM KCl, 1.8 mM $CaCl_2$, 1 mM $MgCl_2$, 10 mM glucose, 0.1% bovine serum albumin, and 15 mM HEPES, pH 7.6) on culture in 125Na-sf or in Fura-2/ECS solution with $CaCl_2$ omitted upon culture in 0Ca-sf. After incubation of 30 min at 37°C, the cell suspension was diluted 10-fold with either ECS or 0CaECS, incubated for an additional 30 min, collected by centrifugation, washed, and resuspended in fresh ECS/0CaECS. Aliquots from Fura-2-loaded cell suspensions were washed twice immediately before fluorescence measurements were performed at 37°C in a mechanically stirred cuvette using a spectrofluorimeter (8100; SLM Aminco, Rochester, NY). For measurements of free $[Ca^{2+}]_i$, the excitation wavelength alternated between 340 and 380 nm every second, whereas emission was monitored at 510 nm. Calibration was done by cell lysis using Triton X-100 in the presence of saturating calcium concentrations followed by addition of EGTA. Free $[Ca^{2+}]_i$ was calculated using equations by Grynkiewicz et al. (1985), with a K_d value of 224 nM for Ca^{2+} binding to Fura-2.

pH_i/BCECF Measurements. HEK/hERG cells were treated overnight with 100 nM digoxin or 25 mM lactic acid in either 125Na-sf or Ch-sf medium. Cells were harvested and resuspended for 30 min at 37°C in the dark in ECS solution containing approximately 2.5 μM BCECF-AM, the pH indicator (Invitrogen). After dye loading, cells were washed twice and resuspended in fresh ECS.

BCECF-loaded cell suspensions were measured at 37°C using an SLM 8100 spectrofluorimeter. For pH_i measurements, the excitation wavelength alternated between 440 and 490 nm, with emission being monitored at 535 nm. In situ calibration was performed using 10 μM nigericin (Sigma-Aldrich) in high K^+ buffer solutions and was nearly linear over the pH range 6.5 to 7.5 (Paradiso et al., 1984; Nilsson et al., 2003).

$[Na^+]_i$/SBFI Measurements. HEK/hERG cells were treated overnight with increasing concentrations of digoxin in 125Na-sf. Cells were harvested and resuspended for 60 min at room temperature in ECS solution containing 10 μM SBFI-AM, the ratiometric Na^+ indicator (Invitrogen), and 0.2% Pluronic F-127 to enhance dye loading (Harootunian et al., 1989). After loading, the cell suspension was washed to remove excess dye and incubated for an additional 30 min to increase de-esterification of the AM dye. Aliquots from SBFI-loaded cell suspensions were analyzed at 37°C using an SLM 8100 spectrofluorimeter, with excitation wavelengths of 340 and 380 nm, whereas emission was monitored at 500 nm. In situ calibration was performed using 1 to 10 μM gramicidin and 100 μM ouabain in extracellular solutions of variable $[Na^+]$. Calibration curves were fitted to Michaelis-Menten equations as described below for $[K^+]_i$/PBFI measurements (Kasner and Ganz, 1992).

$[K^+]_i$/PBFI Measurements. For $[K^+]_i$ measurements, we used the ratiometric potassium indicator PBFI, which is only 1.5-fold more selective for K^+ than for Na^+ (Minta and Tsien, 1989). Therefore, measurements were performed in HEK/hERG cells incubated overnight in NMDG-sf medium (residual $[Na^+]_{ex}$, approximately 5 mM) with increasing concentrations of digoxin. Cells were harvested and resuspended for 60 min at room temperature in ECS solution in which Na^+ had been substituted with equimolar NMDG and that contained 10 μM PBFI-AM (Invitrogen) together with 0.2% Pluronic F-127 for enhanced dye loading. After loading, cell suspensions were washed to remove excess dye and incubated for an additional 30 min to increase de-esterification of the AM dye. Aliquots from PBFI-loaded cell suspensions were analyzed at 37°C using an SLM 8100 spectrofluorimeter, with excitation wavelengths of 340 and 380 nm, whereas emission was monitored at 500 nm. In situ calibration was performed using 10 μM gramicidin in extracellular solutions of variable $[K^+]$. Calibration solutions were prepared by mixing appropriate volumes of a high $[K^+]$ solution containing 120 mM potassium gluconate, 30 mM KCl, 10 mM glucose, and 10 mM HEPES, pH 7.4, with a zero $[K^+]$ solution in which 120 mM lithium gluconate and 30 mM LiCl replaced K^+ salts (Kiedrowski, 1999). To determine intracellular potassium concentrations, calibration curves were fitted to Michaelis-Menten equations of the following form (Kasner and Ganz, 1992): $I_{340}/I_{380} = I_{max}([K^+]_i/[K^+]_I + K_m) + I_0$, where I_{340}/I_{380} is the fluorescence ratio measured at different $[K^+]$; I_0 is the minimal fluorescence ratio measured with $[K^+]$ approaching zero; the sum of I_{max} and I_0 is the maximal fluorescence ratio obtained with saturating $[K^+]$ concentrations; and K_m is the Michaelis-Menten constant, which reflects the affinity of PBFI for $[K^+]$.

Sucrose Gradients and Blue Native-PAGE

HEK/hERG (digoxin treated/untreated controls) cells were lysed in digitonin lysis buffer containing 150 mM NaCl, 10 mM Tris, pH 7.4, 1% digitonin, and protease inhibitors (Complete; Roche Diagnostics). Soluble material (400–800 μg of total protein) was layered onto 15 to 45% sucrose gradients (150 mM NaCl, 10 mM Tris, pH 7.4, and 0.1% digitonin). Gradients were made using BIOCOMP model 117 Gradient Mate (BIOCOMP, Fredericton, NB, Canada) according to the manufacturer's instructions and centrifuged in a SW50.1 rotor (Beckman Coulter, Fullerton, CA) at 48,000 rpm for 16 to 18 h at 4°C, with brakes fully applied. After centrifugation, 275-μl fractions were collected manually from the top of each gradient. Aliquots of individual fractions (150 μl) were concentrated using PAGEprep Protein Clean-Up and Enrichment kit (Pierce Chemical) before loading onto a SDS-PAGE gel for Western blotting. Alternatively, aliquots of gradient fractions were loaded on blue native-PAGE gels. BN-PAGE was carried out as described previously (Greger et al., 2003), with the following modifications. We used 4 to 12% ready-made Bis-Tris gels (Invitrogen) that lack aminocaproic acid. After running gels (5–6 h, starting at 75 V with 25-V increments every 60–90 min, at 4°C), proteins were transferred onto Hybond-P membrane (GE Healthcare) in 50 mM Tris, 380 mM glycine, and 20% methanol (40 mA overnight at 4°C). Before probing with antibodies, membranes were briefly washed in methanol to remove excess Coomassie G-250. Native-gel molecular weight markers (GE Healthcare) were used for calibration. For BN-PAGE, we used hERG WT HA_{ex} protein, which could be detected with high sensitivity using rat anti-HA 3F10 antibody (Roche Diagnostics).

Cellular Electrophysiology

HEK/hERG cells were recorded using patch pipettes filled with 100 mM K-aspartate, 20 mM KCl, 2 mM $MgCl_2$, 1 mM $CaCl_2$, 10 mM EGTA, and 10 mM HEPES, pH 7.2. The extracellular recording solution was 140 mM NaCl, 5 mM KCl, 1 mM $MgCl_2$, 1.8 mM $CaCl_2$, 10 mM HEPES, and 10 mM glucose, pH 7.4. Some hERG mutant channels with ultrafast current inactivation were recorded in the presence of 140 mM KCl as an equimolar substituent for NaCl in the extracellular solution (Gang and Zhang, 2006). To study long-term drug effects on currents, cardiac glycosides were added for 16 to 20 h (overnight) before recording. Stock solutions were prepared in dimethyl sulfoxide. PCLAMP software and an Axon 200B patch-clamp amplifier (Molecular Devices, Sunnyvale, CA) were used for the generation of voltage-clamp protocols and data acquisition. To analyze current densities, membrane capacitance was measured using the analog compensation circuit of the patch-clamp amplifier. All current recordings were performed at room temperature (20–22°C).

Data Analysis

Data are expressed as mean ± S.E.M. of n experiments or cells studied. Differences between means were usually tested using either a two-tailed Student's t test or single factor analysis of variance followed by a two-tailed Dunnett's test to determine whether multiple treatment groups were significantly different from control. P values <0.05 were considered statistically significant. Concentration-response relationships were fit to Hill equations of the following form: $I_{drug}/I_{control} = 1/\{1 + ([D]/IC_{50})^{nH}\}$, where I indicates current or image densities, [D] is the drug concentration, n_H is the Hill coefficient, and IC_{50} is the drug concentration necessary for half-maximal inhibition.

Results

Is Na^+/K^+ Pump-Mediated Signal Transduction Responsible for hERG Trafficking Inhibition? Although cardiac glycosides are best known for their ability to inhibit Na^+/K^+ pumps with high potency and specificity at the level of the cell surface membrane, pump inhibition is also known to trigger additional intracellular signals, including an increase in Src-mediated tyrosine phosphorylation, generation of radical oxygen species (ROS), activation of the Ras/MAP kinase cascade as well as changes in gene expression (Pierre and Xie, 2006). To test whether cardiac glycoside-induced changes in protein phosphorylation and/or gene expression may link pump inhibition at the cell surface to hERG misfolding in the ER, we used specific inhibitors of signal transduction pathways connected to Na^+/K^+ pump inhibition. Figure 1 shows Western blot experiments in which stably transfected HEK/hERG WT cells were incubated overnight with increasing concentrations of digoxin or ouabain in the presence of either 5 mM N-acetyl cysteine (NAC), an antioxidant, to inhibit ROS production (Xie et al., 1999), 10 μM PD98059, the mitogen-activated protein (MAP) kinase ki-

nase (MEK) inhibitor to disrupt the Ras/MAP kinase cascade (Kometiani et al., 1998), or 2.5 μg/ml actinomycin D to suppress gene transcription. As described, both digoxin and ouabain reduce expression of the mature, fully glycosylated cell surface form of hERG (fg hERG; 155 kDa) in a concentration-dependent manner as a consequence of hERG trafficking inhibition (Wang et al., 2007). Here, we show that suppression of hERG processing by digoxin/ouabain was not reversed by coincubation with either NAC or PD98059. Coincubation with actinomycin D reduced the amount of immature, ER resident core-glycosylated hERG (cg hERG; 135 kDa) because of the expected decrease in hERG transcription; yet, the digoxin-induced reduction of fg hERG was not affected (Fig. 1A). To further explore other cell signaling pathways as a mechanism underlying digoxin-induced hERG misfolding, we tested a large number of additional compounds for their potential to modify disruption of hERG trafficking. These compounds included genistein (50 μM) to inhibit Src-mediated tyrosine phosphorylation (Liu et al., 2000); U0126 (1 and 10 μM) to interfere with MEK1 and -2 function in the Ras/ERK MAP kinase cascade (Kometiani et al., 1998; Dmitrieva and Doris, 2003); SP600125 (0.1 and 1 μM), an inhibitor of c-Jun NH_2-terminal kinase (Kometiani et al., 2005); SB203580 (1 and 10 μM), an inhibitor of p38 MAP kinase; H89 (1 and 10 μM) and KT5720 (0.1 and 1 μM), two different protein kinase A inhibitors; and olomucine (1, 10, and 50 μM), an inhibitor of p34cdk1/cyclin B kinase (Lin et al., 2004). In addition, we transiently transfected constitutively activated Raf (caRaf/RafBXB) as well as a dominant-negative Raf (dnRaf/Raf301) into stable HEK/hERG cells in an attempt to interfere with Ras/MAP kinase signaling using nonpharmacological means (Kometiani et al., 1998). However, none of these interventions was able to significantly attenuate or block the disruption of hERG trafficking by cardiac glycosides (Fig. 1B).

Modification of Intracellular Na^+ and K^+ Ion Gradients by Na^+/K^+ Pump Inhibition Affects hERG Processing in the ER. Because it seemed unlikely that signal transduction events triggered by pump inhibition were responsible for disruption of hERG trafficking per se, we explored whether drug-induced changes in intracellular ion composition could drive hERG misfolding. In most cell types, it is thought that Na^+/K^+ pump inhibition produces an increase of intracellular $[Na^+]$, which is translated into elevated intracellular free $[Ca^{2+}]$ levels via activation of the Na^+/Ca^{2+} exchanger. To address the putative effects of changes in $[Ca^{2+}]_i$ on hERG folding and processing, we exposed stably transfected HEK/hERG cells overnight to increasing concentrations of ouabain in a serum-based medium with or without 2.5 mM EDTA (Fig. 2A). In addition, we coincubated ouabain-treated HEK/hERG cells with the membrane-permeable calcium buffer BAPTA AM (10 and 25 μM) to minimize any increase in $[Ca^{2+}]_i$ (data not shown). We found that chelation of neither $[Ca^{2+}]_{ex}$ nor BAPTA AM attenuated hERG trafficking inhibition by cardiac glycosides. Next, we incubated HEK/hERG cells overnight with digoxin in a defined serum-free salt solution with 1 mM Ca^{2+} present (125Na-sf, physiological control) or in a nominally Ca^{2+}-free solution (0Ca-sf) (Fig. 2A). Detection of the fully glycosylated cell surface form of hERG on Western blots was reduced by digoxin treatment, with an IC_{50} value of 42.0 ± 3.2 nM in 125Na-sf and 35.5 ± 7.3 nM in 0Ca-sf (Hill coefficient, 1.75 and n = 3; Fig. 2B). To complement Western blot data, we analyzed hERG tail current amplitudes on return to −50 mV after maximal activation of hERG at +60 mV. After overnight incubation in 0Ca-sf, current amplitudes were reduced from 70.9 ± 5.5 to 1.4 ± 0.9 pA/pF and 1.1 ± 0.2 pA/pF when measured in electrophysiological experiments with standard recording solutions (see *Materials and Methods*), upon exposure to 100 or 300 nM digoxin, respectively (n = 7). Under control conditions in 125Na-sf, we observed a similar reduction in tail current amplitudes from 76.5 ± 9.0 to 2.5 ± 0.3 pA/pF and 2.2 ± 2.2 pA/pF with 100 or 300 nM digoxin, respectively (n = 6–15; Supplemental Fig. S1). Although removal of calcium ions did not affect current density under control conditions (Supplemental Fig. S2) or sensitivity of hERG to digoxin, this does not necessarily preclude changes in cytosolic $[Ca^{2+}]$. Therefore, we used the ratiometric fluorescent dye Fura-2 to directly measure intracellular free Ca^{2+} concentrations in HEK/hERG cells as a function of

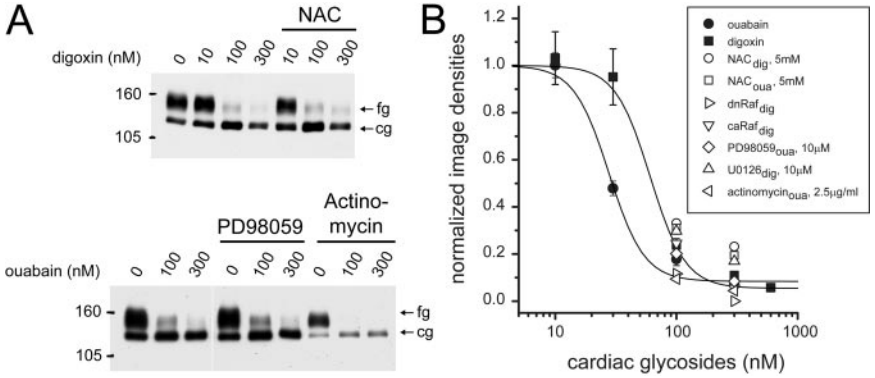

Fig. 1. Inhibition of Na^+/K^+ pump signaling does not prevent block of hERG trafficking by cardiac glycosides. A, Western blots showing effects of overnight treatment with increasing concentrations of digoxin or ouabain on hERG protein stably expressed in HEK293 cells. On Western blots, both digoxin and ouabain reduce the fully glycosylated, mature 160-kDa form of hERG (fg) in a concentration-dependent manner. (cg) indicates core-glycosylated, ER-resident 135-kDa form of hERG. Cardiac glycoside-induced inhibition of hERG trafficking was not affected by coincubation with 5 mM NAC to reduce ROS production, 10 μM PD98059, the MAP kinase kinase (MEK/ERK) inhibitor, or 2.5 μg/ml actinomycin to prevent changes in gene expression. B, concentration-dependent reduction of fully glycosylated, 160-kDa form of hERG after long term-exposure to digoxin or ouabain. Overlaid are coincubations with various inhibitors of Na^+/K^+ pump signaling. In experiments with dominant-negative Raf-1(dnRaf; Raf301) and constitutively active Raf (caRaf; BXB Raf) HEK293 cells were cotransfected with hERG WT(1.5 μg) and either dn- or caRaf (1 μg) before overnight incubation with cardiac glycosides. PD98059 and U0126 were used as inhibitors of MEK1 and MEK2 (ERK1/2).

overnight exposure to digoxin in the presence or absence of extracellular calcium ions. In these experiments, we were not able to detect any significant change in intracellular free $[Ca^{2+}]$ on long-term exposure of HEK/hERG cells to either 100 or 300 nM digoxin, two concentrations that maximally suppressed hERG trafficking as judged from Western blotting or electrophysiological experiments (Supplemental Table S1).

In contrast to $[Ca^{2+}]_i$, overnight incubation with digoxin produced the expected increase in cytosolic $[Na^+]$ after Na^+/K^+ pump inhibition. Using the fluorescent indicator SBFI, we measured a basal $[Na^+]_i$ of 3.9 ± 0.3 mM in HEK/hERG cells. After overnight incubation with 10 or 30 nM digoxin, $[Na^+]_i$ increased to 8.1 ± 0.6 and 61.5 ± 8.1 mM, respectively (n = 3). Our $[Na^+]$ determinations were less precise at digoxin concentrations of 30 nM or higher because of the variability of measurements. Nevertheless, it seems reasonable to assume that overnight exposure to 100 or 300 nM digoxin increased cytosolic Na^+ levels in HEK/hERG cells to at least 80 mM (n = 3; Fig. 3A), which is in line with $[Na^+]_i$ levels reported after Na^+/K^+ pump blockade in a fibroblast cell line (Harootunian et al., 1989).

To investigate the effects of elevated cytosolic $[Na^+]$ on hERG folding, we exposed stably transfected HEK/hERG cells overnight to increasing concentrations of digoxin in a defined, nominally sodium-free salt solution, in which NaCl had been replaced with an equimolar concentration of choline chloride (Ch-sf). On Western blots, disruption of hERG maturation by digoxin was strongly attenuated in the absence of extracellular Na^+ ions (Fig. 3B). Quantitative analysis revealed that suppression of hERG maturation by digoxin was less potent, with an IC_{50} value of 36.0 ± 3.9 nM in 125Na-sf and 352.0 ± 85.6 nM in Ch-sf (n = 3–6; Fig. 3C). To exclude direct effects of choline ions on hERG trafficking, we performed additional experiments using a second serum-free salt solution in which Na^+ ions had been replaced by *N*-methyl-D-glucamine (NMDG-sf). In these experiments, suppression of hERG trafficking by digoxin was less efficient, with an IC_{50} value of 163.6 ± 7.3 nM (n = 3). In addition, dose-response curves were more shallow in the absence of extracellular Na^+, with Hill coefficients being reduced from 2.2 ± 0.5 in 125Na-sf to 1.5 ± 0.1 in NMDG-sf and 1.3 ± 0.4 in Ch-sf solution (n = 3–6; Fig. 3C). In line with our Western analysis, digoxin reduced hERG tail current amplitudes, with IC_{50} values of 49.4 ± 11.1 nM (Hill coefficient fixed at 4; n = 5–15) in 125Na-sf solution and 194.6 ± 0.5 nM in Ch-sf solution (Hill coefficient fixed at 3; n = 8–16; Fig. 3D; Supplemental Fig. S1).

Because removal of extracellular Na^+ ions from incubation media only attenuated digoxin-mediated effects, we reasoned that hERG folding may not be controlled directly by cytosolic Na^+ but regulated indirectly via sodium-dependent changes in intracellular pH or $[K^+]$. To explore the possibility that digoxin-induced pH_i changes may underlie hERG trafficking inhibition, we used the fluorescent dye BCECF to directly measure intracellular pH in HEK/hERG cells as a function of overnight exposure to digoxin. We found that pH_i was not statistically different between control and digoxin-treated HEK/hERG cells, whereas overnight exposure to 25 mM lactic acid significantly acidified the intracellular milieu without any effect on hERG maturation (Supplemental Table S2).

Next, we considered the possibility that the increases in cytosolic $[Na^+]$ observed on Na^+/K^+ pump inhibition are compensated by a decrease in cytosolic $[K^+]$, which could destabilize the selectivity filter and subsequently the entire hERG channel protein (Zhou et al., 2001, 2003; Krishnan et al., 2005). Direct measurements of intracellular K^+ concentrations using the fluorescent indicator PBFI, however, are problematic in high sodium media, because PBFI is only 1.5-fold more selective for K^+ than for Na^+, and we had observed large changes in $[Na^+]_i$ on long-term exposure to digoxin. To overcome this hurdle, we took advantage of the fact that digoxin still inhibited hERG processing in the absence of extracellular $[Na^+]$, albeit with lower sensitivity (see above). We measured $[K^+]_i$ in HEK/hERG cells after incubation with nominally sodium-free NMDG-sf solution and determined a basal $[K^+]_i$ of 58.4 ± 1.6 mM (n = 3), which is considerably lower than the expected physiological concentrations of 120–140 mM. One explanation may be that HEK/hERG cells had been exposed overnight to NMDG-sf before $[K^+]_i$ measurements, which may have lead to an accumulation of intracellular NMDG and a corresponding loss of cytosolic K^+ even under control conditions. In addition, the calibration curve for PBFI measurements is extremely shallow

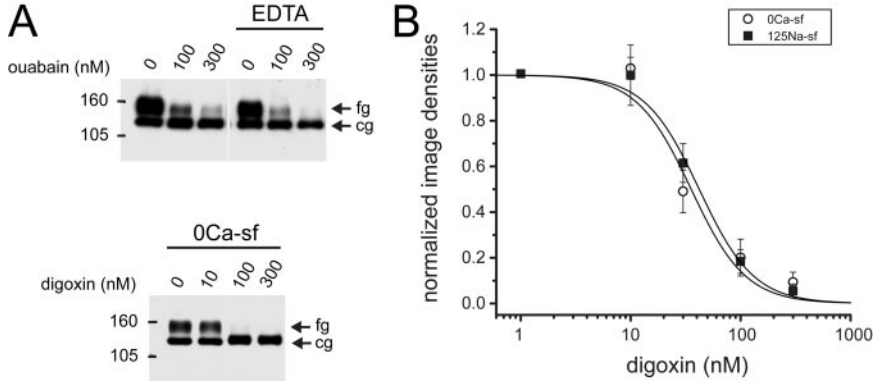

Fig. 2. Removal of extracellular $[Ca^{2+}]$ does not prevent block of hERG trafficking by cardiac glycosides. A, Western blots showing effects of overnight treatment with increasing concentrations of digoxin in the absence and presence of 2.5 mM EDTA (in DMEM/10% fetal bovine serum) on hERG protein stably expressed in HEK293 cells. To assess the effects of extracellular calcium on hERG trafficking more directly, HEK/hERG cells were cultured overnight in a calcium- and serum-free salt solution (0Ca-sf). Cardiac glycoside-induced inhibition of hERG trafficking was not affected by incubation with a nominally calcium-free incubation medium. B, concentration-dependent reduction of fg, 160-kDa form of hERG after long term-exposure to digoxin in serum-free (125Na-sf) and serum-/calcium-free (0Ca-sf) incubation medium. IC_{50} value was 42.0 ± 3.2 nM for incubation in 125Na-sf and 35.5 ± 7.3 nM for 0Ca-sf (Hill coefficient was 1.75; n = 3–6).

at higher $[K^+]$, which makes measurements less precise (Fig. 4A). When intracellular $[K^+]$ was measured as function of overnight exposure to 10, 100, and 300 nM digoxin, $[K^+]_i$ decreased in a concentration-dependent manner from 58.4 ± 1.6 mM to 46.0 ± 7.3, 32.1 ± 3.2, and 13.6 ± 0.7 mM, respectively (n = 3; Fig. 4B).

Assuming that this decrease in $[K^+]_i$ is responsible for inhibition of hERG trafficking by digoxin, we explored whether trafficking may be rescued by stabilizing $[K^+]_i$ at elevated levels via increasing extracellular $[K^+]$. Unfortunately, extracellular K^+ ions are known to compete with cardiac glycosides for one and the same binding site on the Na^+/K^+ pump and may therefore modulate Na^+/K^+ pump activity independently of direct effects of K^+ on hERG folding and trafficking (Palasis et al., 1996). Thus, we depleted intracellular $[K^+]$ in HEK/hERG cells in the absence of cardiac glycosides using the ionophore gramicidin, which forms cation-selective pores. In sodium-free NMDG-sf medium (with 5 mM residual $[K^+]_{ex}$) the fully glycosylated cell surface form of hERG was reduced by approximately 50% after overnight exposure of HEK/hERG cells to 2.5 μM gramicidin, whereas the core-glycosylated form was not affected (Fig. 4C). Gramicidin-induced disruption of hERG trafficking could be reversed by incubation in NMDG-sf media with elevated potassium concentrations. The fully glycosylated cell surface form of hERG could be rescued half-maximally by addition of 13.5 ± 1.1 mM $[K^+]_{ex}$ (Hill coefficient, 2.9 ± 0.6; n = 3–4) and reached a plateau on addition of approximately 30 to 40 mM $[K^+]_{ex}$ (Fig. 4D). Many proteins that are stabilized by K^+ or require K^+ for function are often also activated or stabilized by Rb^+ (Di Cera, 2006). Hence, we determined whether the gramicidin-induced disruption of hERG trafficking could be also restored by incubation with increasing $[Rb^+]_{ex}$. We found that hERG trafficking was restored half-maximally with addition of 10.0 ± 2.4 mM $[Rb^+]_{ex}$ (n = 4; Fig. 4D) similarly to what has been described for $[K^+]_{ex}$ and that levels of the fully glycosylated cell surface form of hERG reached a plateau with approximately 20 mM $[Rb^+]$ present in the extracellular incubation medium.

Rescue of Digoxin-Induced Trafficking Inhibition by Low Incubation Temperatures or the Pharmacological Chaperone Astemizole. Based on observations made with KcsA in which the tetrameric structure of the channel protein seems to be stabilized by conducting ions such as K^+ and Rb^+, we speculated that depletion of intracellular $[K^+]$ by cardiac glycosides may result in destabilization of hERG tetramers, producing incompletely assembled channels that are retained in the ER (Krishnan et al., 2005). Thus, we analyzed the tetrameric assembly of hERG by separating digitonin lysates of HEK/hERG cells incubated in the absence and presence of 300 nM digoxin on 15 to 45% sucrose gradients. We also included brefeldin A in the incubation media to facilitate the quantitative analysis of hERG assembly by preventing complex glycosylation in the Golgi apparatus. Figure 5 shows a Western blot analysis of hERG gradient fractions illustrating the distribution of hERG in two prominent peaks, P1 and P2, with the majority of hERG protein present in P2. Quantitative differences in the distribution of hERG on the sucrose gradient could not be detected as a consequence of drug exposure (n = 3; Fig. 5, A–C). The assembly state of hERG in peaks P1 and P2 was determined directly using BN-PAGE. Several P1 and P2 fractions were separated on BN-gradient gels and analyzed by Western blotting. When the mobility of channel complexes was compared with known molecular weight markers, we found, that hERG was present either as monomer or dimer in P1, whereas in P2 hERG formed tetrameric channel complexes (Fig. 5D).

Because the tetrameric assembly of hERG was preserved in the presence of digoxin, we tested whether drug-induced

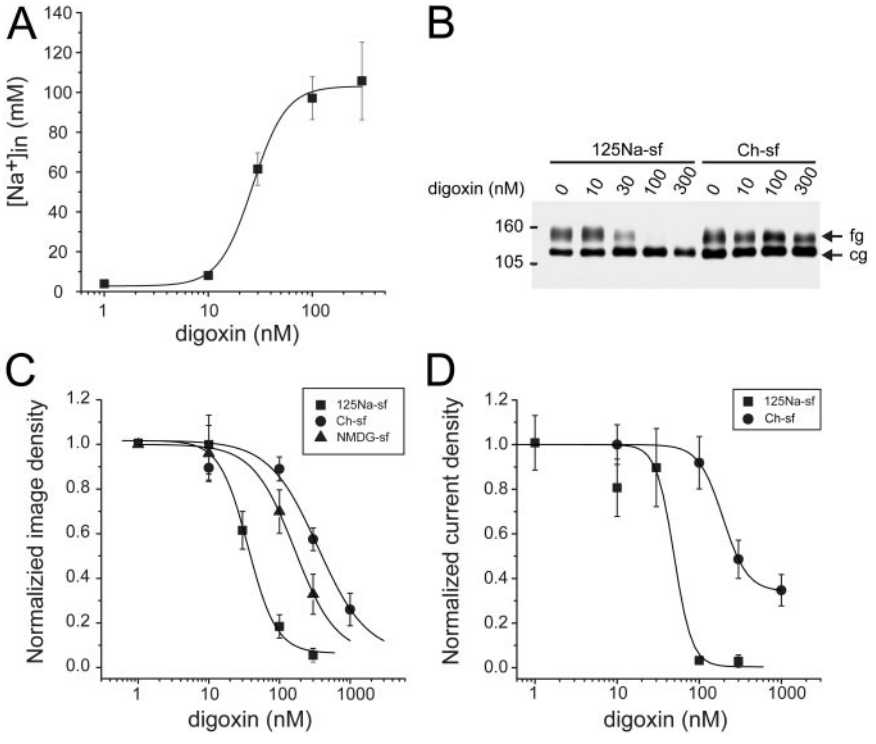

Fig. 3. Removal of extracellular $[Na^+]$ attenuates block of hERG trafficking by cardiac glycosides. A, measurement of intracellular $[Na^+]$ as a function of overnight exposure to increasing concentrations of digoxin (incubation medium, 125Na-sf) using the ratiometric dye SBFI. Intracellular $[Na^+]$ increases from 3.9 ± 0.3 to 105.8 ± 19.5 mM in the presence of 300 nM digoxin (n = 3). B, Western blot showing effects of overnight treatment with increasing concentrations of digoxin in the absence and presence of extracellular $[Na^+]$ on hERG protein stably expressed in HEK293 cells. HEK/hERG cells were cultured overnight in either 125Na-sf or in a low sodium salt solution (Ch-sf) in which extracellular Na^+ has been replaced by choline (residual Na^+, 5 mM). Cardiac glycoside-induced inhibition of hERG trafficking was attenuated by incubation in Ch-sf medium. C, concentration-dependent reduction of fg, 160-kDa form of hERG after long term-exposure to increasing concentrations of digoxin in 125Na-sf, Ch-sf or NMDG-sf, in which extracellular sodium has been replaced by NMDG. IC_{50} values were 36.0 ± 3.85 nM for 125Na-sf, 163.6 ± 7.3 nM for NMDG-sf, and 352.0 ± 85.6 nM for Ch-sf (Hill coefficients were 2.2, 1.5, and 1.26, respectively; n = 3–6). D, concentration-dependent reduction of normalized hERG tail current densities after overnight exposure to digoxin in either 125Na-sf or Ch-sf. Tail currents were recorded on return to −50 mV after a depolarizing voltage step to +60 mV (holding potential, −80 mV). IC_{50} was 49.4 ± 11.1 nM for incubation in 125Na-sf and 194.6 ± 0.5 nM for Ch-sf (Hill coefficients were fixed at 4 and 3, respectively; n = 5–16).

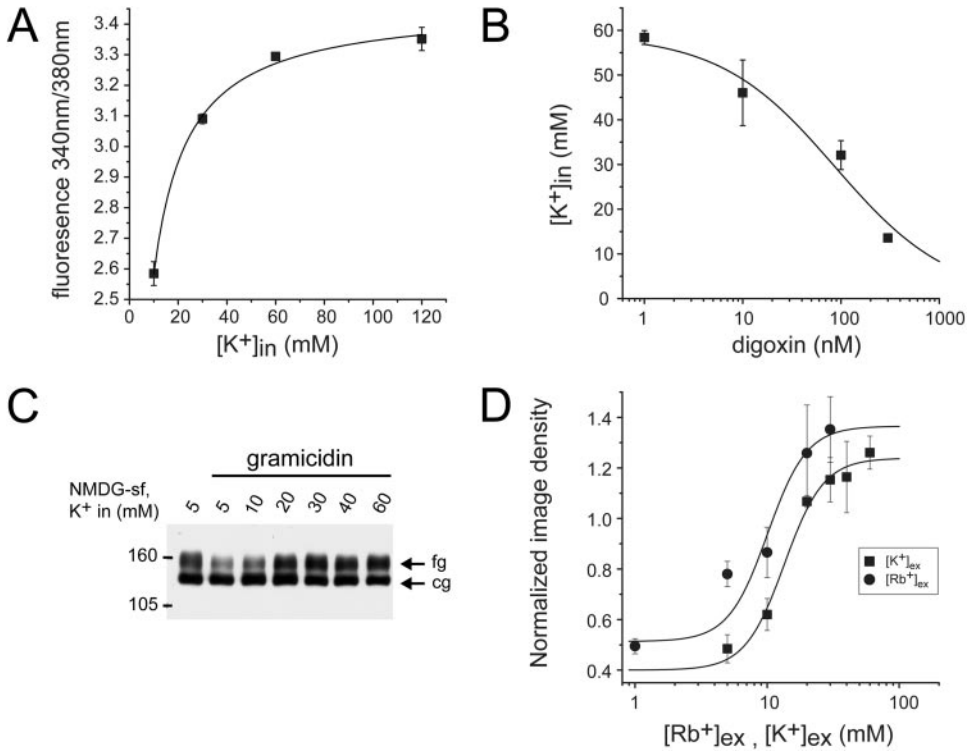

Fig. 4. Loss of intracellular [K^+] initiates block of hERG trafficking by cardiac glycosides. A, calibration curve for the ratiometric dye PBFI showing dependence of 340 nm/380 nm fluorescence ratio on [K^+] in low sodium incubation medium in which sodium ions have been replaced with NMDG (NMDG-sf). Data were fit to Michaelis-Menten equation. Note that the affinity of PBFI for potassium ions (K_m) is approximately 4 mM in the absence of sodium ions in accordance with published data (n = 3). B, measurement of intracellular [K^+] as a function of overnight exposure to increasing concentrations of digoxin (incubation medium, 5K135NMDG-sf) using the ratiometric dye PBFI. Intracellular [K^+] decreases from 58.4 ± 1.6 to 13.6 ± 0.7 mM in the presence of 300 nM digoxin. IC_{50} value was 86.9 ± 6.5 nM (Hill coefficient was 0.74; n = 3). C, Western blot showing effects of overnight treatment with 2.5 μM gramicidin, a cation-selective pore in the presence of increasing concentrations of extracellular K^+ on hERG protein stably expressed in HEK293 cells. HEK/hERG cells were cultured overnight in NMDG-sf or in solutions in which equivalent amounts of NMDG have been replaced by increasing concentrations of K^+. Gramicidin-induced inhibition of hERG trafficking is relieved by increases in extracellular K^+. D, concentration-dependent increase of fg, 160-kDa form of hERG on exposure to increasing $[K^+]_{ex}$ or $[Rb^+]_{ex}$. IC_{50} value was 13.1 ± 1.1 mM for K^+ and 10.0 ± 2.4 mM for Rb^+ (Hill coefficient was 2.9; n = 3–4).

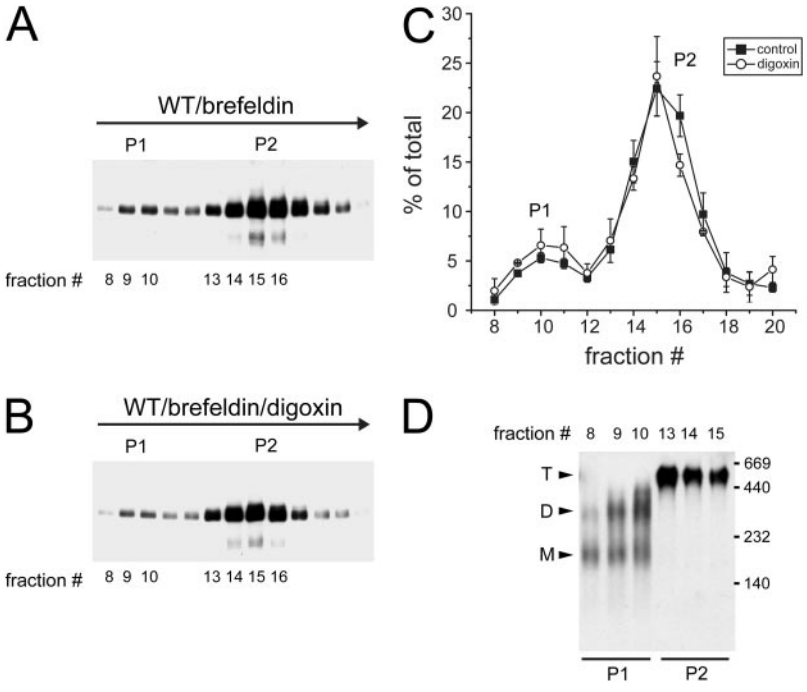

Fig. 5. Long-term exposure to digoxin does not alter tetrameric structure of hERG. A, sedimentation analysis of heterologously expressed hERG WT channels incubated overnight in the presence of 1 μg/ml brefeldin A to inhibit complex glycosylation of the channel protein. Digitonin lysates were separated on 15–45% sucrose gradients. Gradient fractions were analyzed by Western blotting using anti-hERG antibody. The direction of sedimentation is indicated by an arrow. P1 and P2 denote two major hERG peaks. Fraction numbers are indicated below the Western blot. Image densities of gradient fractions were analyzed using a Storm PhosphorImager (GE Healthcare). B, sedimentation analysis of heterologously expressed hERG WT channels incubated overnight in the presence of 1 μg/ml brefeldin A (BFA) and 300 nM digoxin. C, quantification of steady-state sedimentation gradients shown in A and B. Signals from an entire gradient were summed up and set at 100% (total). Individual signals in each fraction were expressed as percentage of total. Major peaks P1 and P2 are indicated (n = 3). D, BN-PAGE showing peak fractions P1 and P2 from a sucrose gradient analyzing heterologous expressed hERG HA_{ex} WT (+BFA) channels. Gradient fractions were taken up in BN loading buffer, separated on a 4 to 12% Bis-Tris gradient gel and analyzed by Western blotting with high-affinity anti-HA antibody (Roche Diagnostics). M, D, and T denote monomer, dimer, and tetramer, respectively. hERG monomers and dimers were present in P1 fractions, whereas P2 fractions consisted entirely of tetramers.

trafficking inhibition could be corrected by stabilizing channel tetramers with low incubation temperature or known pharmacological chaperones such as astemizole. Both interventions have been used successfully in the past to rescue trafficking deficient hERG channel mutants (Ficker et al., 2002). In a first set of Western blot experiments, we incubated HEK/hERG cells with increasing concentrations of digoxin at a low incubation temperature (26°C) and observed that the digoxin effect on hERG maturation was largely abolished (Fig. 6, A and C). To further explore "low temperature" rescue, we analyzed I_{hERG} in HEK/hERG cells exposed overnight to increasing concentrations of digoxin at 26°C. To our surprise, hERG currents decreased from 54.1 ± 8.3 pA/pF under control conditions to 33.1 ± 9.4 and 12.3 ± 2.3 pA/pF on incubation with 100 or 300 nM digoxin, respectively (n = 9–11; Fig. 6D). Similar findings were obtained with astemizole, an antihistamine that blocks WT channels in electrophysiological experiments, with an IC_{50} value of approximately 1 nM. On Western blots, 5 μM astemizole restored hERG maturation in the presence of 100 or 300 nM digoxin to a large extent at 37°C (Fig. 6, B and C). On coincubation with 100 nM digoxin, rescue was half-maximal with 71 ± 27 nM astemizole (n = 3; data not shown). This was significantly higher than the concentration needed for half-maximal block in electrophysiological experiments, indicating that although digoxin-treated hERG channel tetramers provide a binding site for astemizole, they may do so with small structural deviations from the native state. To test whether rescue of hERG trafficking by astemizole may be extended to hERG currents, we performed additional electrophysiological recordings. At −50 mV, we measured fully activated hERG tail current amplitudes of 83.5 ± 6.7 pA/pF (n = 6) under control conditions, 1.5 ± 0.5 pA/pF (n = 5) after overnight incubation with 100 nM digoxin, and 9.8 ± 2.0 pA/pF (n = 8) after overnight coincubation with 100 nM digoxin and 5 μM astemizole after a 1-h washout before recording. We also recorded from HEK/hERG cells incubated solely with 5 μM astemizole and measured tail current amplitudes of 39.1 ± 4.3 pA/pF after a 1-h washout (n = 9; Fig. 6D). From these data, we determined that 5 μM astemizole rescued at most 25% of I_{hERG}, whereas Western blot data seemed to indicate that approximately 65% of the fully glycosylated cell surface protein was rescued. Taken together, these results suggested that long-term exposure to cardiac glycosides produces two distinct effects on hERG: one effect leading to a decrease in conductance and another effect rendering channels trafficking deficient.

Digoxin-Induced Trafficking Defect Is Attenuated by Mutations in the Selectivity Filter of hERG. To identify regions of the channel protein involved in digoxin-mediated trafficking inhibition, we analyzed large truncations of either the N or C terminus of hERG as well as a series of point mutations in transmembrane regions, including D456A, E518A, E519A, E575A, D580A, D591A; D609A, S620T, and G628C/S631C. We found that none of these deletions or point mutants affected inhibition of hERG matu-

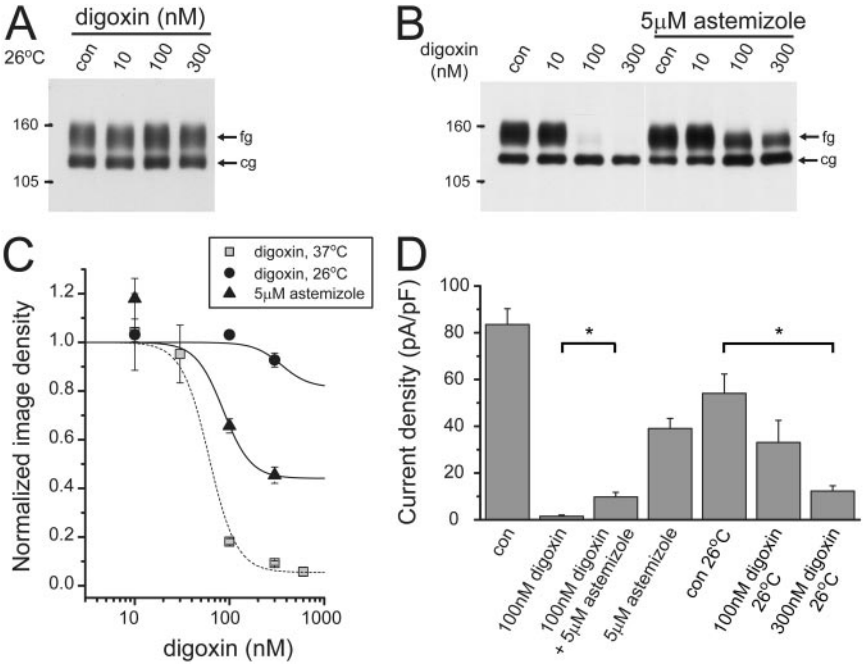

Fig. 6. Rescue of digoxin-induced hERG trafficking block by incubation at low temperature or with the pharmacological chaperone astemizole. A, Western blot showing effects of overnight treatment with increasing concentrations of digoxin at a low incubation temperature of 26°C. Note, that digoxin does not reduce the fg, mature 160-kDa form of hERG (fg) at 26°C. (cg) indicates core-glycosylated ER-resident 135-kDa form of hERG. B, Western blot showing effects of overnight treatment with increasing concentrations of digoxin in the presence and absence of 5 μM astemizole at 37°C. Incubation with astemizole attenuates the hERG trafficking block induced by digoxin. C, quantification of the fg cell surface form of hERG after long-term exposure to increasing concentrations of digoxin at physiological temperature (37°C), at low incubation temperature (26°C; n = 3) and on coincubation with 5 μM astemizole (37°C; n = 3). D, hERG tail current densities measured on return to −50 mV after a depolarizing pulse to +60 mV (holding potential, −80 mV) under control conditions, on overnight incubation with 100 nM digoxin (37°C), 100 nM digoxin + 5 μM astemizole (washout, 1 h), and 5 μM astemizole to determine residual astemizole block after 1-h washout. Note that long-term exposure to 5 μM astemizole significantly increases hERG tail currents reduced by overnight incubation with 100 nM digoxin (t test, $p < 0.05$; n = 6–9). In marked contrast, tail currents were significantly reduced on incubation with 300 nM digoxin (Dunnett's, $p < 0.05$; n = 9–11) at low incubation temperatures (26°C), despite the fact that the fully glycosylated form of hERG was not changed on Western blots.

ration by cardiac glycosides (data not shown). Next, we focused on the selectivity filter, which provides a well recognized binding site for both K^+ and Rb^+, as a target for depletion of $[K^+]_i$ (Zhou et al., 2001; Lockless et al., 2007). We analyzed four different mutations using Western blots and current recordings. On Western blots, hERG F627Y, a mutation in the GFG signature sequence of the selectivity filter, proved to be significantly less sensitive to digoxin than WT or hERG S624A, a mutation at the intracellular end of the selectivity filter (Fig. 7, A and B). In addition, hERG S641A, a mutation in the S6 transmembrane helix with biophysical properties similar to F627Y (Bian et al., 2004), was more resistant to 100 nM digoxin than WT. Finally, we tested hERG S631A, a mutation in the extracellular mouth of the conduction pathway that disrupts C-type inactivation (Zou et al., 1998) and found wild-type sensitivity to digoxin (Fig. 7B). Our Western analysis was closely matched by current recordings from transiently transfected WT or mutant channels on incubation with either 100 or 300 nM digoxin. To account for differences in channel gating, we analyzed maximally activated WT, hERG S624A, and hERG S631A tail currents on return to −50 mV in the presence of 5 mM $[K^+]_{ex}$, whereas both hERG F627Y and S641A tail currents were recorded on return to −80 mV in 140 mM $[K^+]_{ex}$ because of their fast C-type inactivation behavior (Gang and Zhang, 2006). To allow for direct comparison, current amplitudes were normalized. Both hERG F627Y and S641A currents were significantly less sensitive to digoxin than WT channels (Fig. 7C; Supplemental Fig. S3). Taken together, our structure-function analysis points toward the selectivity filter as a region of the channel protein that may be involved in the digoxin/low $[K^+]$-induced disruption of hERG trafficking.

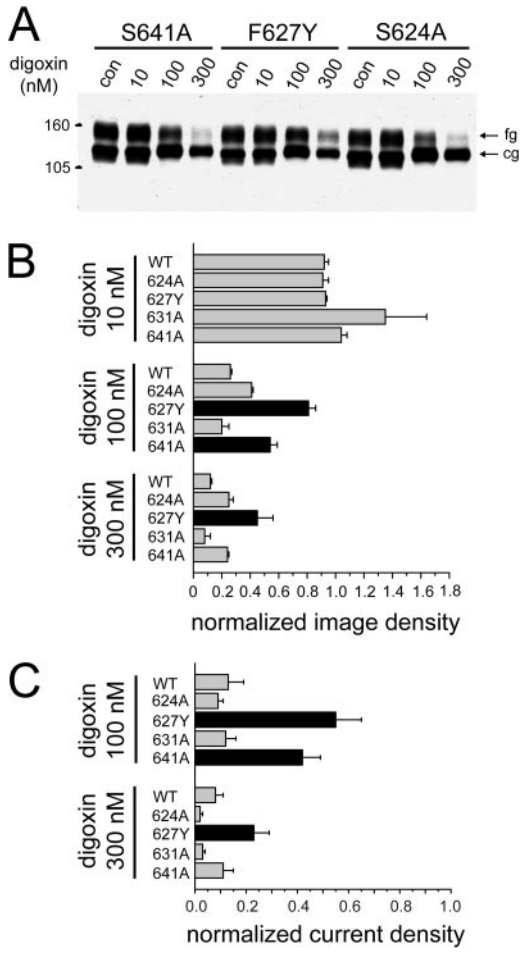

Fig. 7. Mutations in the selectivity filter alter sensitivity of hERG to digoxin induced trafficking inhibition. A, Western blot showing effects of overnight treatment with increasing concentrations of digoxin on hERG S641A, hERG F627Y, and hERG S624A protein transiently expressed in HEK293 cells. (fg) indicates the fully glycosylated, mature 160-kDa form of hERG (fg). (cg) indicates core-glycosylated ER-resident 135-kDa form of hERG. B, quantitative analysis of fg, 160-kDa form of hERG WT, hERG S641A, hERG F627Y, and hERG S624A after long term-exposure to 10, 100, and 300 nM digoxin. Image densities of fully glycosylated protein bands on Western blots were captured using a Storm PhosphoImager (GE Healthcare), quantified, and normalized to untreated controls. Black bars indicate a significant difference between fg-WT and fg-hERG F627Y or fg-hERG S641A on treatment with either 100 or 300 nM digoxin (Dunnett's t test, $p < 0.05$; $n = 3–4$). C, hERG WT, hERG S624A, and hERG S631A currents were activated in the presence of 5 mM $[K^+]_{ex}$ from a holding potential of −80 mV, with a depolarizing pulse to +60 mV (2 s). Tail currents were recorded on return to −50 mV. For hERG F627Y and S641A, tail currents were recorded on return to −80 mV in the presence of 140 mM $[K^+]_{ex}$. Tail current amplitudes were converted into current densities and normalized to amplitudes measured in untreated controls. Black bars indicate a significant difference between WT and hERG F627Y or hERG S641A current densities on exposure to either 100 or 300 nM digoxin (Dunnett's t test, $p < 0.05$; $n = 4–10$).

Discussion

To provide a mechanistic explanation for the disruption of hERG trafficking by cardiac glycosides, we targeted multiple signaling pathways thought to be activated by Na^+/K^+ pump inhibition. However, we were not able to establish any link between these signaling pathways and hERG trafficking inhibition. Of course, these experiments are limited by the specificity of the pharmacological inhibitors used, as well as by the possibility that a pathway, not yet connected to pump inhibition, may be important. In contrast, we have found compelling evidence that hERG trafficking inhibition is mediated via cardiac glycoside-induced changes in intracellular ion composition, in particular, that hERG channels are stabilized for export from the ER by K^+ or Rb^+ ions.

In our experiments, we profiled changes in intracellular proton/cation concentrations and found that neither pH_i nor $[Ca^{2+}]_i$ was altered on long-term exposure to cardiac glycosides. In contrast, Na^+/K^+ pump inhibition increased $[Na^+]_i$ in a dose-dependent manner, and hERG trafficking inhibition was attenuated but not abolished in Na^+-depleted incubation media. Finally, increases in $[Na^+]_i$ were accompanied by a corresponding decrease in $[K^+]_i$, a cation known to stabilize K^+ channel structure (Krishna et al., 2005). To test directly for effects of K^+ on hERG trafficking, we developed an assay that allowed us to deplete $[K^+]_i$ in the absence of pump inhibition using the pore-forming antibiotic gramicidin in nominally Na^+-free media. Using this assay, we were able to show that depletion of $[K^+]_i$ was sufficient to disrupt hERG trafficking and that trafficking could be restored upon incubation with K^+-enriched, Na^+-free media. Likewise, hERG trafficking was rescued on incubation with Rb^+ ions, which are similar in size to K^+, and activate many proteins that depend on K^+ for proper function (Di Cera, 2006). Taken together, our experiments suggested that a K^+-activated protein may play an important role in the processing and export pathway of hERG or, alternatively, that a potassium-dependent conformational change of hERG may disrupt trafficking.

Putative targets in the export pathway are protein kinases and chaperones with a structural requirement for K^+ binding. One interesting candidate is the cytosolic chaperone heat shock cognate 70, a component of the hERG folding machinery (O'Brien and McKay, 1995; Ficker et al., 2003). Because heat shock cognate 70 is required for folding of most newly synthesized proteins, inhibition via $[K^+]_i$ depletion should affect a large, diverse set of proteins. However, we have shown more recently that disruption of ER export by cardiac glycosides was specific for hERG (Wang et al., 2007). Furthermore, we have shown here that hERG trafficking is restored in the continuous presence of cardiac glycosides by the pharmacological chaperone astemizole (Ficker et al., 2002). Both of these observations indicate that "general" protein processing and export pathways in the ER remain largely intact on long-term exposure to cardiac glycosides.

Thus, we propose that hERG adopts a misfolded, trafficking-deficient conformation on synthesis in the absence of appropriate $[K^+]_i$ concentrations. This implies that the native conformation of hERG is stabilized directly by interaction with K^+. In high-resolution structures of potassium channels, multiple K^+ binding sites have been identified along the conduction pathway including the narrow selectivity filter (Zhou et al., 2001). In fact, the selectivity filter represents a dynamic structure that is stabilized by permeating ions. For example, in the presence of low concentrations of permeating ions, the selectivity filter may assume a distinct, nonconductive conformation (Zhou and MacKinnon, 2003). Structural changes in the selectivity filter have also been associated with C-type inactivation (Cordero-Morales et al., 2007). Furthermore, it has been known for a long time that removal of extracellular K^+ produces a loss of conductance in Shaker K^+ channels, with the structure of the selectivity filter being altered (Loboda et al., 2001).

Thus, the hERG selectivity filter may respond with a similar conformational change to $[K^+]_i$ depletion—either directly after exposure to gramicidin in low sodium media or indirectly upon long-term exposure to cardiac glycosides. This hypothesis is supported by several observations. First, two different permeating ions, K^+ and Rb^+, were able to rescue hERG trafficking. Second, hERG trafficking was stabilized by two mutations in or close to the selectivity filter, hERG F627Y and S641A. hERG F627Y, which reverts the GFG filter sequence of hERG into the GYG signature sequence present in most other potassium channels, is particularly interesting because the amino acid residue in position 627 is thought to participate in a cuff of aromatic residues meant to stabilize the filter region. Therefore, hERG F627Y may provide a first answer as to why cardiac glycosides disrupt hERG trafficking specifically. Finally, low incubation temperature restored hERG trafficking to the cell surface but not conductance, as if many channels were locked in a nonconducting state after being processed in a K^+-depleted intracellular environment. Likewise, rescue experiments with astemizole at physiological temperature seemed to produce a high percentage of channels at the cell surface with impaired conductance.

Although our data are compatible with a localized structural rearrangement in the hERG selectivity filter, it is possible that additional K^+ binding sites may exist outside the conduction pathway. Even though this cannot be ruled out, structural data acquired for several potassium channels including Kv1.2 have not provided any evidence for the existence of such sites. It is also possible that the proposed conformational change does not remain localized to the narrow selectivity filter but instead may affect the entire conduction pathway. However, the cavity as well as the external mouth of the channel is not selective for permeating cations. For example, Na^+ interacts with an outer pore site of hERG, with an affinity of approximately 3 mM (Mullins et al., 2002), whereas the cavity of the prototypical KcsA potassium channel is thought to bind Na^+, with an affinity of 80 to 100 mM (Zhou and MacKinnon, 2004). Thus, both of these sites are most likely occupied by Na^+ in the presence of cardiac glycosides, with $[Na^+]_i$ reaching up to 80 mM. However, Na^+ may not be sufficient to stabilize hERG for export from the ER. On the contrary, Na^+ may help clear K^+ ions from their respective binding sites, as judged from much steeper dose-response curves measured for cardiac glycosides in the presence of $[Na^+]_{ex}$. Despite all similarities, it is important to point out that the loss of hERG conductance observed on long-term exposure to cardiac glycosides in rescue experiments seems to be irreversible, whereas structural changes observed in KcsA on exposure to low $[K^+]$ or conduction changes in Shaker channels are considered reversible (Gómez-Lagunas, 1997). Most importantly, hERG WT channels do not adopt a nonconducting state in the absence of conducting K^+ ions. Instead, they conduct Na^+ currents (Gang and Zhang, 2006).

As already mentioned, effects of cardiac glycosides on conductance and trafficking could be separated in rescue experiments. For example, at low incubation temperature nonconducting hERG WT channels were exported from the ER. This suggests that the underlying structural changes are not easily monitored by cellular quality control mechanisms. The privileged position the selectivity filter holds with respect to cellular quality control mechanisms may provide a plausible explanation as illustrated in an LQT2 filter mutation, hERG G628S, which produces nonconducting channels that reach the cell surface (Sanguinetti et al., 1996). Likewise, it has been shown that the low K^+ filter conformation of KcsA has minimal impact on the overall structure of the channel protein (Zhou and MacKinnon, 2003). At the same time, this raises the intriguing question as to what additional conformational changes hERG channels may undergo on exposure to cardiac glycosides when trafficking is disrupted at physiological temperature. At the moment, we only know that assembly of hERG into channel tetramers is not likely to be affected.

Taken together, we have demonstrated that disruption of hERG trafficking by cardiac glycosides is because of induced misfolding of the channel protein upon synthesis in a low K^+ environment. We propose that during biosynthesis of hERG, permeating ions such as K^+ or Rb^+ establish a conductive filter structure in an initial binding event with millimolar affinity. If occupancy of these sites remains low during synthesis, the selectivity filter misfolds and adopts a nonconductive structure. At physiological temperature, changes in the filter structure trigger additional, more extensive conformational changes that ultimately lead to ER retention. Overall, we present a novel molecular mechanism for drug-induced trafficking inhibition that contrasts sharply with the disruption of hERG trafficking by much better understood 90-kDa heat shock protein inhibitors, which abolish the interaction

with an accessory protein essential for channel maturation and export (Ficker et al., 2003). The proposed mechanism may also help us understand why clinical use of cardiac glycosides has rarely been associated with QT prolongation and torsades de pointes arrhythmias. The simplest explanation may be that intracellular K^+ concentrations low enough for inhibition of hERG trafficking can be found only in cardiomyocytes undergoing apoptosis or possibly in extreme cases of intoxication with cardiac glycosides but not at the low plasma concentrations reached during therapy with digoxin or digitoxin.

Acknowledgments

We thank G. Robertson (University of Wisconsin, Madison, WI) for providing hERG 1B cDNA and M. Sanguinetti (University of Utah, Salt Lake City, UT) as well as S. Zhang (Queen's University, Kingston, ON, Canada) for several different mutant hERG channel cDNAs.

References

Bian JS, Cui J, Melman Y, and McDonald TV (2004) S641 contributes HERG K^+ channel inactivation. *Cell Biochem Biophys* **41:**25–40.
Cordes JS, Sun Z, Lloyd DB, Bradley JA, Opsahl AC, Tengowski MW, Chen X, and Zhou J (2005) Pentamidine reduces hERG expression to prolong the QT interval. *Br J Pharmacol* **145:**15–23.
Cordero-Morales JF, Jogini V, Lewis A, Vásquez V, Cortes DM, Roux B, and Perozo E (2007) Molecular driving forces determining potassium channel slow inactivation. *Nat Struct Mol Biol* **14:**1062–1069.
Di Cera E (2006) A structural perspective on enzymes activated by monovalent cations. *J Biol Chem* **281:**1305–1308.
Dmitrieva RI and Doris PA (2003) Ouabain is a promoter of growth and activator of ERK1/2 in ouabain-resistant rat renal epithelial cells. *J Biol Chem* **278:**28160–28166.
Ficker E, Obejero-Paz CA, Zhao S, and Brown AM (2002) The binding site for channel blockers that rescue misprocessed human long QT syndrome type 2 *ether-a-gogo*-related gene (hERG) mutations. *J Biol Chem* **277:**4989–4998.
Ficker E, Dennis AT, Wang L, and Brown AM (2003) Role of the cytosolic chaperones Hsp70 and Hsp90 in maturation of the cardiac potassium channel HERG. *Circ Res* **92:**e87–100.
Ficker E, Kuryshev YA, Dennis AT, Obejero-Paz C, Wang L, Hawryluk P, Wible BA, and Brown AM (2004) Mechanisms of arsenic-induced prolongation of cardiac repolarization. *Mol Pharmacol* **66:**33–44.
Gang H and Zhang S (2006) Na^+ permeation and block of hERG potassium channels. *J Gen Physiol* **128:**55–71.
Gómez-Lagunas F (1997) Shaker B K^+ conductance in Na^+ solutions lacking K^+ ions: a remarkable stable non-conducting state produced by membrane depolarizations. *J Physiol* **499:**3–15.
Greger IH, Khatri L, Kong X, and Ziff EB (2003) AMPA receptor tetramerization is mediated by Q/R editing. *Neuron* **40:**763–774.
Grynkiewicz G, Poenie M, and Tsien RY (1985) A new generation of Ca^{2+} indicators with greatly improved fluorescence properties. *J Biol Chem* **260:**3440–3450.
Guo J, Massaeli H, Li W, Xu J, Luo T, Shaw J, Kirshenbaum LA, and Zhang S (2007) Identification of I_{Kr} and its trafficking disruption induced by probucol in cultured neonatal rat cardiomyocytes. *J Pharmacol Exp Ther* **321:**911–920.
Harootunian AT, Kao JP, Eckert BK, and Tsien RY (1989) Fluorescence ratio imaging of cytosolic free Na^+ in individual fibroblasts and lymphocytes. *J Biol Chem* **264:**19458–19467.
Kasner SE and Ganz MB (1992) Regulation of intracellular potassium in mesangial cells: a fluorescence analysis using the dye, PBFI. *Am J Physiol* **262:**F462–F467.
Kiedrowski L (1999) *N*-Methyl-D-aspartate excitotoxicity: relationships among plasma membrane potential, Na^+/Ca^{2+} exchange, mitochondrial Ca^{2+} overload, and cytoplasmic concentrations of Ca^{2+}, H^+, and K^+. *Mol Pharmacol* **56:**619–632.
Kometiani P, Li J, Gnudi L, Kahn BB, Askari A, and Xie Z (1998) Multiple signal transduction pathways link Na^+/K^+-ATPase to growth-related genes in cardiac myocytes. *J Biol Chem* **273:**15249–15256.
Kometiani P, Liu L, and Askari A (2005) Digitalis-induced signaling by Na^+/K^+-ATPase in human breast cancer cells. *Mol Pharmacol* **67:**929–936.
Krishnan MN, Bingham JP, Lee SH, Trombley P, and Moczydlowski E (2005) Functional role and affinity of inorganic cations in stabilizing the tetrameric structure of the KcsA K+ channel. *J Gen Physiol* **126:**271–283.
Kuryshev YA, Ficker E, Wang L, Hawryluk P, Dennis AT, Wible BA, Brown AM, Kang J, Chen XL, Sawamura K, et al. (2005) Pentamidine-induced long QT syndrome and block of hERG trafficking. *J Pharmacol Exp Ther* **312:**316–323.
Lin H, Juang JL, and Wang PS (2004) Involvement of Cdk5/p25 in digoxin-triggered prostate cancer cell apoptosis. *J Biol Chem* **279:**29302–29307.
Liu J, Tian J, Haas M, Shapiro JI, Askari A, and Xie Z (2000) Ouabain interaction with cardiac Na^+/K^+-ATPase initiates signal cascades independent of changes in intracellular Na^+ and Ca^{2+} concentrations. *J Biol Chem* **275:**27838–27844.
Loboda A, Melishchuk A, and Armstrong CM (2001) Dilated and defunct K channels in the absence of K^+. *Biophys J* **80:**2704–2714.
Lockless SW, Zhou M, and MacKinnon R. (2007) Structural and thermodynamic properties of selective ion binding in a K^+ channel. *PLoS Biol* **5:**e121.
Minta A and Tsien RY (1989) Fluorescent indicators for cytosolic sodium. *J Biol Chem* **264:**19449–19457.
Mullins FM, Stepanovic SZ, Desai RR, George AL Jr, and Balser JR (2002) Extracellular sodium interacts with the HERG channel at an outer pore site. *J Gen Physiol* **120:**517–537.
Nilsson C, Kågedal K, Johansson U, and Ollinger K (2003) Analysis of cytosolic and lysosomal pH in apoptotic cells by flow cytometry. *Methods Cell Sci* **25:**185–194.
O'Brien MC and McKay DB (1995) How potassium affects the activity of the molecular chaperone Hsp70. *J Biol Chem* **270:**2247–2250.
Palasis M, Kuntzweiler TA, Argüello JM, and Lingrel JB (1996) Ouabain interactions with the H5–H6 hairpin of the Na,K-ATPase reveal a possible inhibition mechanism via the cation binding domain. *J Biol Chem* **271:**14176–14182.
Paradiso AM, Tsien RY, and Machen TE (1984) Na+-H+ exchange in gastric glands as measured with a cytoplasmic-trapped, fluorescent pH indicator. *Proc Natl Acad Sci U S A* **81:**7436–7440.
Pierre SV and Xie Z (2006) The Na,K-ATPase receptor complex: its organization and membership. *Cell Biochem Biophys* **46:**303–316.
Rajamani S, Eckhardt LL, Valdivia CR, Klemens CA, Gillman BM, Anderson CL, Holzem KM, Delisle BP, Anson BD, Makielski JC, et al. (2006) Drug-induced long QT syndrome: hERG K^+ channel block and disruption of protein trafficking by fluoxetine and norfluoxetine. *Br J Pharmacol* **149:**481–489.
Sanguinetti MC, Curran ME, Spector PS, and Keating MT (1996) Spectrum of HERG K^+-channel dysfunction in an inherited arrhythmia. *Proc Natl Acad Sci U S A* **93:**2208–2212.
Sanguinetti MC and Mitcheson JS (2005) Predicting drug-hERG channel interactions that cause acquired long QT syndrome. *Trends Pharmacol Sci* **26:**119–124.
Sanguinetti MC and Tristani-Firouzi M. (2006) hERG potassium channels and cardiac arrhythmia. *Nature* **440:**463–469.
Takemasa H, Nagatomo T, Abe H, Kawakami K, Igarashi T, Tsurugi T, Kabashima N, Tamura M, Okazaki M, Delisle BP, et al. (2007) Coexistence of hERG current block and disruption of protein trafficking in ketoconazole-induced long QT syndrome. *Br J Pharmacol* **153:**439–447.
van der Heyden MA, Smits ME, and Vos MA (2007) Drugs and trafficking of ion channels: a new pro-arrhythmic threat on the horizon? *Br J Pharmacol* **153:**406–409.
Wang L, Wible BA, Wan X, and Ficker E (2007) Cardiac glycosides as novel inhibitors of human *ether-a-gogo*-related gene channel trafficking. *J Pharmacol Exp Ther* **320:**525–534.
Wible BA, Hawryluk P, Ficker E, Kuryshev YA, Kirsch G, and Brown AM (2005) HERG-Lite: a novel comprehensive high-throughput screen for drug-induced hERG risk. *J Pharmacol Toxicol Methods* **52:**136–145.
Xie Z, Kometiani P, Liu J, Li J, Shapiro JI, and Askari A (1999) Intracellular reactive oxygen species mediate the linkage of Na^+/K^+-ATPase to hypertrophy and its marker genes in cardiac myocytes. *J Biol Chem* **274:**19323–19328.
Zhou Y, Morais-Cabral JH, Kaufman A, and MacKinnon R. (2001) Chemistry of ion coordination and hydration revealed by a K^+ channel Fab complex at 2.0 Å resolution. *Nature* **414:**43–48.
Zhou Y and MacKinnon R (2003) The occupancy of ions in the K+ selectivity filter: charge balance and coupling of ion binding to a protein conformational change underlie high conduction rates. *J Mol Biol* **333:**965–975.
Zhou Y and MacKinnon R (2004) Ion binding affinity in the cavity of the KcsA potassium channel. *Biochemistry* **43:**4978–4982.
Zou A, Xu QP, and Sanguinetti MC (1998) A mutation in the pore region of HERG K+ channels expressed in *Xenopus* oocytes reduces rectification by shifting the voltage dependence of inactivation. *J Physiol* **509:**129–137.

Address correspondence to: Dr. Eckhard Ficker, Rammelkamp Center, MetroHealth Medical Center, 2500 MetroHealth Dr., Cleveland, OH 44109. E-mail: eficker@metrohealth.org